Pancreatic Neuroendocrine Tumors and EMT Behavior are Driven by the CSC Marker DCLK1

Yu Ikezono[1,2], Hironori Koga[1,2], Jun Akiba[3], Mitsuhiko Abe[1,2], Takafumi Yoshida[1,2], Fumitaka Wada[1,2], Toru Nakamura[1,2], Hideki Iwamoto[1,2], Atsutaka Masuda[1,2], Takahiko Sakaue[1,2], Hirohisa Yano[3], Osamu Tsuruta[1], and Takuji Torimura[1,2]

[1]Division of Gastroenterology, Department of Medicine, Kurume University School of Medicine
[2]Liver Cancer Research Division, Research Center for Innovative Cancer Therapy, Kurume University
[3]Department of Pathology, Kurume University School of Medicine

Corresponding author
Hironori Koga, M.D., Ph.D.
Professor
Division of Gastroenterology and Translational Medicine,
Department of Medicine,
Kurume University School of Medicine
67 Asahi-machi, Kurume 830-0011, Japan
Email: hirokoga@med.kurume-u.ac.jp
Tel: +81-942-31-7561
Fax: +81-942-34-2623

Running title: DCLK1 Defines PNET Behavior

Abbreviations: DCLK1, doublecortin-like kinase 1; CSC, cancer stem cell; NET, neuroendocrine tumor; EMT, epithelial-mesenchymal transition; FAK, focal adhesion kinase; ERK, extracellular signal-regulated kinase; siRNA, small interfering RNA; EV, empty vector; mTOR, mammalian target of rapamycin

Keywords: epithelial-mesenchymal transition, cancer stem cell, NET, FAK, SLUG

Electronic word count: 4438 (excluding words in References)
Figures: 7
Tables: 4
Supplementary Figures: 5

Conflict of interest statement: All authors disclose no conflicts.

Funding Support: This work was supported by Pancreas Research Foundation of Japan and JSPS KAKENHI (Grant no. 15K19355).

Authors' contributions: YI and HK participated in study conception and design, acquisition of data, interpretation of data, and drafting of manuscript. AJ, HY, and OT provided tissue samples and pathological information. MA, TY, and TN participated in analysis and interpretation of data. FW, HI, AM, TS, and TT participated in critical discussion.

ABSTRACT

Doublecortin-like kinase 1 (DCLK1), a marker for intestinal and pancreatic cancer stem cells, is highly expressed in neuroblastomas. This study was conducted to assess DCLK1 expression levels in pancreatic neuroendocrine tumor (PNET) tissues and to explore the roles of this molecule in clinical tissue from multiple PNET patients, cells (BON1, QGP1, and CM), and tumor xenografts. Immunohistochemically, all PNET tissues highly and diffusely expressed DCLK1 as a full-length isoform, identical to that detected in primary liver NETs. A DCLK1-overexpressing PNET cell line (QGP1-DCLK1) exhibited epithelial-mesenchymal transition (EMT)-related gene signatures and robust upregulation of Slug (SNAI2), N-Cadherin (CDH2), and Vimentin (VIM) was validated by real-time PCR and immunoblotting. QGP1-DCLK1 cells had increased cell migration in a wound-healing assay and formed significantly larger xenograft tumors in nude mice. The factors involved in the formation of the fast-growing tumors included: p-FAK (on Tyr925), p-ERK1/2, p-AKT, Paxillin, and Cyclin D1 which upon knockdown or pharmacological inhibition of DCLK1 abolished the expression of these molecules. In conclusion, robust and ubiquitous expression of DCLK1 was first demonstrated here in human PNET tissue specimens and cells. DCLK1 characterized the PNET cell behavior, inducing p-FAK/SLUG-mediated EMT. These findings suggest the possibility of developing novel therapeutic strategies against PNETs by targeting DCLK1.

IMPLICATIONS

Evidence here reveals that human PNETs diffusely and robustly express the cancer stem cell marker DCLK1, which drives SLUG-mediated EMT, and suggests that NETs share biological features for druggable targets with other tumors, including neuroblastoma that also highly expresses DCLK1.

1. INTRODUCTION

Although neuroendocrine tumors (NETs) are considered rare tumors, the number of patients with these tumors is gradually increasing worldwide [1-3]. NETs, previously called “carcinoid or benign carcinoma” [4], grow slowly; however, they have metastatic potential, and are categorized as malignant neoplasms [5]. In addition, a study of 310 patients who underwent resection of pancreatic NETs (PNETs) also showed high rates of lymph node metastasis (36.8%) and distant metastasis (20.3%) [6]. Such highly metastatic potential, despite slow tumor growth, is one of the most important features of NETs, including PNETs [7]. Although molecular-targeted drugs have been used to treat PNETs, such as everolimus and sunitinib [8,9], the critical target molecules responsible for its aggressiveness have yet to be determined.

Doublecortin-like kinase 1 (DCLK1) is a microtubule-associated protein that plays key roles in the regulation of neural cell differentiation, migration, and apoptosis during embryonic development [10-12]. Accumulating evidence suggests that DCLK1 is a marker of intestinal and pancreatic stem cells and cancer stem cells (CSCs); thus, it is attracting much attention from both gastroenterologists and oncologists [13-18]. In animal models with xenografted tumors of colon cancer and pancreatic cancer cells, gene silencing of DCLK1 decreased the tumor size [15,17,19]. In another study, it was shown that DCLK1 was involved in not only tumor growth but also invasion and migration [20]. The possible mechanisms underlying the tumor-promoting role of DCLK1 include downregulation of tumor-suppressing microRNA expression, induction of vascular endothelial growth factor receptor and epithelial-mesenchymal transition (EMT)-related factors [17,19,21], and activation of the oncogenic gene *C-MYC* in tumor cells [22]. However, the precise mechanism has not been elucidated.

Recently, we demonstrated strong expression of DCLK1 in rectal NETs [23], which encouraged us to investigate its possible expression in other NETs, including PNETs. Here, we demonstrate DCLK1 expression in both human tissues and a cell line derived from PNETs and reveal its crucial function in the regulation of EMT.

2. MATERIALS AND METHODS

2.1. Patients and tumor tissues

Fifteen patients (8 males and 7 females) with PNETs were enrolled in this study. Four primary liver NET (LNET) tissues were also used as pathological controls, and two of the four LNET tissues were subjected to both western blot analysis and immunohistochemistry for DCLK1. The patients’ tumors were surgically resected between 1997 and 2012 at Kurume University Hospital. Informed consent to participate in the study was obtained from all patients in accordance with the principles stated in the Declaration of Helsinki and the guidelines of the Ethical Committee of

Kurume University (study registration no. 13149; Committee Chair, Kensei Nagata). The mean age of the patients with PNET was 56 years (range, 17 years–80 years). The diagnosis of NET was made by at least two pathologists independently according to the new WHO guidelines for NET [24]. The average diameter of the PNETs was 30.2 mm (range, 12 mm–93 mm). Histologically, nine PNETs were graded as G1, and six were graded as G2. Three PNETs were endocrinologically functional. Distant metastasis or lymph node metastasis was detected in eight cases with PNET (Table 1).

2.2. Cell lines and culture conditions

The human PNET cell lines BON1 [25], QGP1, and CM were used in this study. BON1 was a kind gift from Professor B. Lankat-Buttgereit (Marburg, Germany). QGP1, a somatostatin-secreting cell line [26], was purchased from the Health Science Research Resource Bank (Japan Health Sciences Foundation, Osaka, Japan). CM, an insulin-secreting line [27], was obtained from Professor Paolo Pozzilli (Rome, Italy). All cell lines were grown in DMEM (Wako, Tokyo, Japan) supplemented with 10% heat-inactivated (56°C, 30 minutes) fetal bovine serum (BioWest, Nuaill, France), 100 units/mL penicillin, and 100 μg/mL streptomycin (Nacalai Tesque, Kyoto, Japan) in a humidified atmosphere containing 5% CO_2 at 37°C.

2.3. Immunohistochemistry and staining score

Immunohistochemistry was performed as previously reported [23]. The intensity of DCLK1 staining was scored on a scale of 0 to 3, in which 0 is negative staining, 1 is weakly positive staining, 2 is moderately positive staining, and 3 is strongly positive staining. The signal-positive area was scored on a scale of 0 to 2, in which 0 is positive staining in 0–20% of cells; 1 is positive staining in 21–60% of cells; and 2 is positive staining in 61–100% of cells. If the total score was greater than or equal to 2, it was judged as positive (Table 2). The antibodies used for immunohistochemistry and western blotting are listed in Table 3.

2.4. Western blotting

Cells and homogenized liver NET tissues were lysed with RIPA buffer (Pierce, Rockford, IL) containing Protease Inhibitor Cocktail (Nacalai Tesque) and Halt Phosphatase Inhibitor Cocktail (Pierce). Protein concentrations were measured using the BCA Protein Assay Kit (Pierce). Samples containing 25 μg of protein were separated on 8% or 10% sodium dodecyl sulfate (SDS)-polyacrylamide gels and then transferred to equilibrated polyvinylidene difluoride membranes (Bio-Rad, Hercules, CA). After blocking with 5% non-fat milk, the membranes were incubated with diluted primary antibodies overnight at 4°C. The bound antibodies were detected with horseradish peroxidase (HRP)-labeled secondary antibodies using ECL Plus Western

Blotting Detection Reagents (Amersham Pharmacia Biotech, Buckinghamshire, UK). Positive signals from the target proteins were visualized using an image analyzer (LAS-4000; Fujifilm, Tokyo, Japan). Densitometric analysis of the signals was performed using Multi Gauge software, version 3.0 (Fujifilm).

2.5. Overexpression of DCLK1

A *DCLK1*-expressing plasmid (RC217050) and a control plasmid (RC208006) were obtained from OriGene Technologies, Inc. (Rockville, MD). To generate stable transfectants, QGP1 cells and BON1 cells were transfected with the *DCLK1* cDNA or the empty vector using TransIT-LT1 (Mirus, Madison, WI) according to the manufacturer's instructions. After transfection, DCLK1-overexpressing clones (QGP1-DCLK1 and BON1-DCLK1) were selected with 400 μg/mL G418 (Nacalai Tesque). Mock-transfected cells (QGP1-EV and BON1-EV) were similarly selected with G418 as control clones.

2.6. Gene silencing of DCLK1 *by siRNA*

DCLK1-targeting and non-targeting (NT) siRNAs were purchased from Thermo Fisher Scientific, Inc. (Waltham, MA). Focal adhesion kinase *(FAK)*-targeting siRNA and paired NT siRNAs were obtained from Santa Cruz Biotechnology, Inc. (Santa Cruz, CA). The cells were transfected with these siRNAs using DharmaFECT (Dharmacon, Lafayette, CO) according to the manufacturer's protocol.

2.7. Wound-healing assay

Cells were seeded (6.0×10^4) and grown in 35-mm dishes containing DMEM until confluence. A single scratch was made on the cell surface with a sterile 10-μL pipette tip. Perpendicular marks were made to standardize the viewing fields. Wound healing was monitored, and the distance between the edges of the scratched line was measured at 5 points under a microscope over 48 h.

2.8. cDNA microarray

2.8.1. Total RNA isolation

Total RNA was isolated from QGP1-DCLK1 and QGP1-EV cells using TRIzol Reagent (Thermo Fisher Scientific) and purified using the SV Total RNA Isolation System (Promega Corporation, Madison, WI) according to the manufacturer's instructions. RNA samples were quantified using an ND-1000 spectrophotometer (NanoDrop Technologies, Wilmington, DE), and RNA quality was confirmed with the Experion System (Bio-Rad).

2.8.2. Gene expression microarrays

cRNA was amplified, labeled, and hybridized to a 60K Agilent 60-mer oligomicroarray

according to the manufacturer's instructions. All hybridized microarray slides were scanned with an Agilent scanner. Relative hybridization intensities and background hybridization values were calculated using Agilent Feature Extraction Software (9.5.1.1).

2.8.3. Data analysis and filter criteria

Raw signal intensities and Flags for each probe were calculated from the hybridization intensities (gProcessedSignal) and spot information (gIsSaturated, etc.), according to the procedures recommended by Agilent. (Flag criteria in GeneSpring Software. Absent (A): "Feature is not positive and significant" and "Feature is not above background;" Marginal (M): "Feature is not Uniform," "Feature is Saturated," and "Feature is a population outlier;" Present (P): others.) The raw signal intensities of the samples were normalized using a quantile algorithm with the preprocessCore library package [28] in Bioconductor [29]. We selected probes that called a "P" flag in two samples. To identify upregulated or downregulated genes, we calculated Z-scores [30] and ratios (non-log-scaled fold-change) from the normalized signal intensities of each probe to compare the control and experimental samples. Then, we established the following criteria for regulated genes: Z-score ≥ 2.0 and ratio ≥ 1.5-fold for upregulated genes and Z-score ≤ -2.0 and ratio ≤ 0.66 for down-regulated genes.

2.9. Real-time quantitative PCR (qPCR) analysis

RNA was extracted from cells using TRIzol, and 1 μg of total RNA was reverse transcribed using the TaqMan Reverse Transcription (RT) Reagent kit (Applied Biosystems, Foster City, CA) according to the manufacturer's instructions. qRT–PCR was performed on a 7500 Fast Real Time PCR System (Applied Biosystems) using TaqMan Universal PCR Master Mix (Applied Biosystems). The pre-designed TaqMan probes for the genes of interest were as follows: *DCLK1* (Assay ID, Hs00178027_m1), *SLUG/SNAI2* (Hs00161904_m1), *N-CADHERIN/CDH2* (Hs00362037_m1), *E-CADHERIN/CDH1* (Hs01023894_m1), and *VIMENTIN* (Hs00958111_m1). Gene expression relative to *GAPDH* (Hs02758991_g1) was evaluated according to the ΔΔ-CT method using StepOne Software 2.0 (Applied Biosystems).

2.10. Sphere formation assay

QGP-DCLK1 and QGP-EV cells were seeded (at 1.2×10^4 per well) in ultra-low attachment 6-well plates (Corning, NY) and grown for up to 48 days. Then, the area of the cell spheres was measured using a microscope (BZ-X700) equipped with digital cell counting software (KEYENCE, Osaka, Japan).

2.11. Xenograft model

QGP-DCLK1 and QGP-EV cells (2.5×10^6 per mouse) were subcutaneously injected into the

back of 5-week-old male BALB/c athymic nude mice (n = 10 for each cell line; Clea Japan, Osaka, Japan). Tumor size was measured weekly in two orthogonal directions using calipers, and tumor volume (mm^3) was estimated using the equation length × $(width)^2$ × 0.5. At 42 days after tumor cell inoculation, the mice were sacrificed, and the tumors were resected. The tumor tissues were subjected to hematoxylin and eosin (HE) staining, immunohistochemistry, and western blotting. The average number of mitotic figures (dividing tumor cell nuclei) per high-power field was quantified by counting the figures in six randomly selected fields. All animal experiments were conducted in accordance with the NIH Guidelines for the Care and Use of Laboratory Animals and were approved by the Animal Care and Use Committee of the University of Kurume.

2.12. Functional inhibition of DCLK1

After functional inhibition of DCLK1 by using LRRK2-IN-1 (Calbiochem, San Diego, CA) and XMD 8-92 (Tocris Bioscience, Minneapolis, MN), the molecular changes in treated cells were assessed [22,31,32].

2.13. Statistical analysis

Statistical significance was assessed by the Mann-Whitney U test using StatView 5.0 J software (SAS Institute Inc., Cary, NC). P values less than 0.05 were considered statistically significant.

3. RESULTS

3.1. DCLK1 is highly expressed in PNETs

DCLK1 was diffusely expressed in the cytoplasm of tumor cells in PNET tissues (Fig. 1, Supplementary Fig. S1). All PNET tissues included in the study were positive for DCLK1, although they were not always positive for other common NET markers, such as CHROMOGRANIN A, CD56, and SYNAPTOPHYSIN (Table 4). There was no significant relationship between the DCLK1 staining score and tumor characteristics, including grade, size, presence of endocrine function, and presence of metastasis. Further, there was no significant difference in DCLK1 staining score between primary site (pancreas) and metastatic sites (lymph nodes) in four of eight cases with metastasis (Supplementary Fig. S2). It is known that DCLK1 has four isoforms, two full-length isoforms (80–82 kDa) and two short isoforms (45–50 kDa). The short isoforms lack the N-terminal doublecortin domains, which are the binding sites for microtubules [33]. Importantly, the structural differences among the isoforms of DCLK1 lead to distinct functions [34,35]. Therefore, we initially tried to identify which isoform was expressed in human NET tissues, and found that only the full-length isoform of DCLK1 was clearly expressed

in human primary liver NET (LNET) tissues (Supplementary Fig. S3A). Immunohistochemically, high expression of DCLK1 was detected in four cases with LNET by using the same antibody, suggesting that DCLK1 in LNET tissues was full-length isoform (Supplementary Fig. S3B). Such full-length isoform of DCLK1 was also expressed in the human PNET cell line CM, but not in the other cell lines (BON1 and QGP1) (Fig. 1G). These findings strongly suggested that the used antibody could detect 82 kDa isoform of DCLK1, which was ubiquitously expressed in NET tissues, including PNET and LNET.

3.2. Overexpression of DCLK1 induces EMT

Overexpression of full-length DCLK1 in QGP1-DCLK1 cells was confirmed by western blotting (Fig. 2A). The cell shape changed from round to polygonal and spindle, that was morphologically reminiscent of EMT (Fig. 2B). In addition, the migration ability of these cells was clearly increased in the wound-healing assay (Fig. 2C, D). Conversely, the wound healing speed of *DCLK1*-silenced CM cells was retarded (Fig. 2E, F, G). We then explored the genes involved in the DCLK1-induced EMT, focusing on EMT-associated transcription factors, including *SNAIL* and *SLUG*, by cDNA microarray. The results showed that *SLUG (SNAI2)* expression was robustly upregulated in QGP1-DCLK1 cells, in concert with the remarkable upregulation in *VIM* (*VIMENTIN*) and *TGFB3* (*Transforming Growth Factor Beta 3*) (Supplementary Fig. 4S). *SLUG* upregulation was reproduced in the qPCR analysis, which also showed upregulated expression of two other mesenchymal markers, *VIMENTIN* and *N-CADHERIN* (Fig. 3A). However, the expression of *E-CADHERIN*, an epithelial marker, was not always downregulated in these cells (Fig. 3A). These transcriptional changes were also confirmed at the protein level in not only QGP1-DCLK1 cells but also BON1-DCLK1 cells (Fig. 3B). Because cancer cells with EMT characteristics are prone to sphere formation, sphere-forming ability was semi-quantitatively evaluated with a digital microscope. As expected, QGP1-DCLK1 cells formed significantly more spheres than the control cells (Supplementary Fig. S5A, B). In addition, QGP1-DCLK1 cells showed slight higher cell proliferation *in vitro*, but the difference did not reach a statistical significance.

3.3. DCLK1-overexpressing PNET cell xenograft tumors grow faster

QGP1-DCLK1 cells formed significantly larger xenograft tumors than QGP1-EV cells (Fig. 4A, B, C), suggesting that they had higher proliferative ability *in vivo*. Indeed, a significantly higher frequency of mitosis was observed in QGP1-DCLK1 tumor tissues stained with HE than in QGP1-EV tumor tissues (Fig. 4D, E).

3.4. DCLK1 induces EMT-related characteristics, and tyrosine (Tyr)^{925}-phosphrylated (p-) FAK is

involved

Western blotting showed that the expression of the EMT regulator SLUG was increased in a representative QGP1-DCLK1 tumor tissue (Fig. 4F). Because QGP1-DCLK1 cells showed high migration potential (Fig. 2C, D), we focused on the expression levels of FAK and its downstream molecules, including PAXILLIN, ERK1/2, AKT, and CYCLIN D1. Notably, Tyr^{925}-p-FAK, but not Tyr^{397}-p-FAK, was highly expressed in the QGP1-DCLK1 tumor tissues, which was accompanied by increased expression of PAXILLIN, p-ERK1/2, p-AKT, and CYCLIN D1 (Fig. 4F). Then, we confirmed significant upregulation of both SLUG and Tyr^{925}-p-FAK in all QGP1-DCLK1 tumors studied (n=5 for each group) by immunohistochemistry (Fig. 4G with graphs for immunostaining scores).

3.5. Silencing DCLK1 *by siRNA*

Knockdown of *DCLK1* with an siRNA restored the alterations in the above-mentioned EMT-associated proteins and CYCLIN D1 in QGP1-DCLK1 cells *in vitro* (Fig. 5A). This trend was also confirmed in CM cells, in which the expression of Tyr^{925}-p-FAK and SLUG was constitutively high (Fig. 5B).

3.6. Tyr^{925}-p-FAK induces EMT

To determine the hierarchal relationship between FAK and SLUG, *FAK* was silenced in QGP1-DCLK1 cells. In *FAK*-silenced QGP1-DCLK1 cells, SLUG was lost upon loss of FAK (Fig. 6A). This finding suggested that FAK was upstream of SLUG. Of note, in the next experiment using 1 μM of LRRK2-IN-1, an inhibitor of DCLK1, it was suggested that loss of SLUG was through loss of Tyr^{925}-p-FAK in QGP1-DCLK1 cells, whose expression level of total FAK was not altered (Fig. 6B). In addition, affecting DCLK1 activity by using another small molecule XMD 8-92 resulted in decreased expressions of both Tyr^{925}-p-FAK and SLUG in a dosage-dependent manner, in not only QGP1-DCLK1 cells but also CM cells (Fig. 6C).

4. DISCUSSION

The important findings of this study are as follows: 1) human PNET tissues and the PNET cell line CM robustly expressed DCLK1, 2) DCLK1-overexpressing PNET cells exhibited EMT characteristics, which were highlighted by SLUG upregulation, and 3) mechanistically, upregulated SLUG expression was under the control of Tyr^{925}-p-FAK.

Diffuse and robust expression of DCLK1 in human PNET tissues is a novel finding, when compared with DCLK1 expression patterns in a recent report on primary and metastatic pancreatic cancer tissues [20]. In pancreatic cancer tissues, the CSC marker DCLK1 was often

expressed in metastatic sites, including the liver and lung, whereas it was rarely expressed in primary tumor sites [20]. Such findings are reasonable because the population of CSCs should be small; thus, DCLK1-positive cells would be barely detectable in clinically resected primary cancer tissues, even though the tissues were derived from metastatic lesions. Thus, diffuse and robust expression of DCLK1 seems to be a unique characteristic of human PNET tissues; however, it may be a universal trait of NET because a similar expression pattern was also demonstrated in rectal NET tissues [23]. Such diffuse, strong expression of DCLK1 in NETs may explain their clinical features, such as high metastatic potential despite their early developmental stage [7]. The mechanism underlying robust DCLK1 expression remains to be elucidated. In the immunohistochemical analysis, DCLK1 staining scores did not predict patient prognosis. To validate this, additional studies including larger numbers of cases are needed. In contrast to the clear DCLK1 positivity in all tested PNET tissues, two of the three human PNET cell lines were negative for DCLK1. The reason for this was not clarified in this study; however, full-length DCLK1-negative clones may have been incidentally selected in the establishment of the BON1 and QGP1 cell lines.

Comprehensive analysis of the DCLK1-overexpressing PNET cells showed that SLUG is a core factor involved in the DCLK1-induced EMT. This is consistent with previous findings demonstrating a similar type of EMT in colon and pancreatic cancer cells [20,21]. This similarity suggests that one of the crucial functions of DCLK1 is to induce EMT independent of cell type. Although the causative role of DCLK1 in SLUG-mediated EMT in PNET cells was not fully clarified in this study, we showed that Tyr^{925}-p-FAK, but not Tyr^{397}-p-FAK, was involved in SLUG-mediated EMT in DCLK1-overexpressing PNET cells. Indeed, it is known that FAK phosphorylation at Tyr^{925} preferentially induces EMT via growth factor receptor-bound protein 2 and downstream activation of the RAS and ERK cascade [36-39]. In contrast, phosphorylation of FAK at Tyr^{397} promotes autophosphorylation of this site, relaying extended phosphorylation at other N-terminal phosphorylation sites, including Tyr^{407}, Tyr^{576}, and Tyr^{577} [37,38], and contributing to the physiological development of organs. In this context, we suggest that DCLK1 and Tyr^{925}-p-FAK-mediated EMT involving p-ERK1/2 and SLUG upregulation plays a critical role in determining tumor cell behavior in PNETs [40]. Such activation of FAK in the DCLK1-overexpressing PNET cell line might also contribute to the increase in tumor size and cellular proliferation through upregulating the cell cycle driver CYCLIN D1.

It is well known that SRC phosphorylates FAK at both Tyr^{397} and Tyr^{925} [37,38], although it is not yet understood how these distinct phosphorylations are so tightly regulated. Of note, SRC is abundantly expressed in PNET and is involved in its cell adhesion and migration [41]. Thus, we speculate that DCLK1 may interact with SRC to preferentially phosphorylate Tyr^{925} (Fig. 7). From a therapeutic point of view, abundant expression of FAK in PNET is attractive [42]. In a previous

study, it was demonstrated that inactivation of FAK, coupled with inhibition of mTOR by everolimus, led to increased apoptosis of PNET cells by preventing feedback activation of AKT [42]. Future investigations on how DCLK1 precisely regulates the site-specific phosphorylation of FAK by SRC may provide insights into more druggable targets in PNETs.

5. ACKNOWLEDGEMENTS

We thank Yasuko Imamura and Masako Hayakawa for technical assistance.

6. REFERENCES

1. Yao JC, Hassan M, Phan A, Dagohoy C, Leary C, Mares JE, et al. One hundred years after "carcinoid": epidemiology of and prognostic factors for neuroendocrine tumors in 35,825 cases in the United States. J Clin Oncol. 2008;26:3063-72.

2. Ito T, Igarashi H, Nakamura K, Sasano H, Okusaka T, Takano K, et al. Epidemiological trends of pancreatic and gastrointestinal neuroendocrine tumors in Japan: a nationwide survey analysis. J Gastroenterol. 2015;50:58-64.

3. Ito T, Tanaka M, Sasano H, Osamura YR, Sasaki I, Kimura W, et al. Preliminary results of a Japanese nationwide survey of neuroendocrine gastrointestinal tumors. J Gastroenterol. 2007;42:497-500.

4. Oberndorfer S: Tumoren des Dunndarms. Frankf Z Pathol 1:426-432. Tumoren des Dunndarms. Frankf Z Pathol. 1907;1:426-32.

5. Soga J. Carcinoids and their variant endocrinomas. An analysis of 11842 reported cases. J Exp Clin Cancer Res. 2003;22:517-30.

6. Fischer L, Bergmann F, Schimmack S, Hinz U, Priess S, Muller-Stich BP, et al. Outcome of surgery for pancreatic neuroendocrine neoplasms. Br J Surg. 2014;101:1405-12.

7. Warner RR. Enteroendocrine tumors other than carcinoid: a review of clinically significant advances. Gastroenterology. 2005;128:1668-84.

8. Yao JC, Shah MH, Ito T, Bohas CL, Wolin EM, Van Cutsem E, et al. Everolimus for advanced pancreatic neuroendocrine tumors. N Engl J Med. 2011;364:514-23.

9. Raymond E, Dahan L, Raoul JL, Bang YJ, Borbath I, Lombard-Bohas C, et al. Sunitinib malate for the treatment of pancreatic neuroendocrine tumors. N Engl J Med. 2011;364:501-13.

10. Shu T, Tseng HC, Sapir T, Stern P, Zhou Y, Sanada K, et al. Doublecortin-like kinase controls neurogenesis by regulating mitotic spindles and M phase progression. Neuron. 2006;49:25-39.

11. Koizumi H, Tanaka T, Gleeson JG. Doublecortin-like kinase functions with doublecortin to mediate fiber tract decussation and neuronal migration. Neuron. 2006;49:55-66.

12. Koizumi H, Higginbotham H, Poon T, Tanaka T, Brinkman BC, Gleeson JG. Doublecortin maintains bipolar shape and nuclear translocation during migration in the adult forebrain. Nat Neurosci. 2006;9:779-86.

13. Giannakis M, Stappenbeck TS, Mills JC, Leip DG, Lovett M, Clifton SW, et al. Molecular properties of adult mouse gastric and intestinal epithelial progenitors in their niches. J Biol Chem. 2006;281:11292-300.

14. May R, Sureban SM, Lightfoot SA, Hoskins AB, Brackett DJ, Postier RG, et al. Identification of a novel putative pancreatic stem/progenitor cell marker DCAMKL-1 in normal mouse pancreas. Am J Physiol Gastrointest Liver Physiol. 2010;299:G303-10.

15. Nakanishi Y, Seno H, Fukuoka A, Ueo T, Yamaga Y, Maruno T, et al. Dclk1 distinguishes

between tumor and normal stem cells in the intestine. Nat Genet. 2013;45:98-103.

16. Bailey JM, Alsina J, Rasheed ZA, McAllister FM, Fu YY, Plentz R, et al. DCLK1 marks a morphologically distinct subpopulation of cells with stem cell properties in preinvasive pancreatic cancer. Gastroenterology. 2014;146:245-56.

17. Sureban SM, May R, Ramalingam S, Subramaniam D, Natarajan G, Anant S, et al. Selective blockade of DCAMKL-1 results in tumor growth arrest by a Let-7a MicroRNA-dependent mechanism. Gastroenterology. 2009;137:649-59, 59 e1-2.

18. Westphalen CB, Takemoto Y, Tanaka T, Macchini M, Jiang Z, Renz BW, et al. Dclk1 Defines Quiescent Pancreatic Progenitors that Promote Injury-Induced Regeneration and Tumorigenesis. Cell Stem Cell. 2016;18:441-55.

19. Sureban SM, May R, Qu D, Weygant N, Chandrakesan P, Ali N, et al. DCLK1 regulates pluripotency and angiogenic factors via microRNA-dependent mechanisms in pancreatic cancer. PLoS One. 2013;8:e73940.

20. Ito H, Tanaka S, Akiyama Y, Shimada S, Adikrisna R, Matsumura S, et al. Dominant expression of DCLK1 in human pancreatic cancer stem cells accelerates tumor invasion and metastasis. PLoS One. 2016;11:e0146564.

21. Sureban SM, May R, Lightfoot SA, Hoskins AB, Lerner M, Brackett DJ, et al. DCAMKL-1 regulates epithelial-mesenchymal transition in human pancreatic cells through a miR-200a-dependent mechanism. Cancer Res. 2011;71:2328-38.

22. Weygant N, Qu D, Berry WL, May R, Chandrakesan P, Owen DB, et al. Small molecule kinase inhibitor LRRK2-IN-1 demonstrates potent activity against colorectal and pancreatic cancer through inhibition of doublecortin-like kinase 1. Mol Cancer. 2014;13:103.

23. Ikezono YU, Koga H, Abe M, Akiba J, Kawahara A, Yoshida T, et al. High expression of the putative cancer stem cell marker, DCLK1, in rectal neuroendocrine tumors. Oncol Lett. 2015;10:2015-20.

24. Rindi G AR, Bosman FT. Nomenclature and classification of neuroendocrine neoplasms of the digestive system. In: Bosman FT, Carneiro F, Hruban RH, Theise ND, et al., editors. WHO classification of tumors of the digestive system. Lyon: IARC. 2010.

25. Townsend CM, Jr., Ishizuka J, Thompson JC. Studies of growth regulation in a neuroendocrine cell line. Acta Oncol. 1993;32:125-30.

26. Kaku M, Nishiyama T, Yagawa K, Abe M. Establishment of a carcinoembryonic antigen-producing cell line from human pancreatic carcinoma. Gan. 1980;71:596-601.

27. Baroni MG, Cavallo MG, Mark M, Monetini L, Stoehrer B, Pozzilli P. Beta-cell gene expression and functional characterisation of the human insulinoma cell line CM. J Endocrinol. 1999;161:59-68.

28. Bolstad BM, Irizarry RA, Astrand M, Speed TP. A comparison of normalization methods for

high density oligonucleotide array data based on variance and bias. Bioinformatics. 2003;19:185-93.

29. Gentleman RC, Carey VJ, Bates DM, Bolstad B, Dettling M, Dudoit S, et al. Bioconductor: open software development for computational biology and bioinformatics. Genome Biol. 2004;5:R80.

30. Quackenbush J. Microarray data normalization and transformation. Nat Genet. 2002;32 Suppl:496-501.

31. Deng X, Dzamko N, Prescott A, Davies P, Liu Q, Yang Q, et al. Characterization of a selective inhibitor of the Parkinson's disease kinase LRRK2. Nat Chem Biol. 2011;7:203-5.

32. Sureban SM, May R, Weygant N, Qu D, Chandrakesan P, Bannerman-Menson E, et al. XMD8-92 inhibits pancreatic tumor xenograft growth via a DCLK1-dependent mechanism. Cancer Lett. 2014;351:151-61.

33. Engels BM, Schouten TG, van Dullemen J, Gosens I, Vreugdenhil E. Functional differences between two DCLK splice variants. Brain Res Mol Brain Res. 2004;120:103-14.

34. Verissimo CS, Molenaar JJ, Meerman J, Puigvert JC, Lamers F, Koster J, et al. Silencing of the microtubule-associated proteins doublecortin-like and doublecortin-like kinase-long induces apoptosis in neuroblastoma cells. Endocr Relat Cancer. 2010;17:399-414.

35. O'Connell MR, Sarkar S, Luthra GK, Okugawa Y, Toiyama Y, Gajjar AH, et al. Epigenetic changes and alternate promoter usage by human colon cancers for expressing DCLK1-isoforms: Clinical Implications. Sci Rep. 2015;5:14983.

36. Brunton VG, Avizienyte E, Fincham VJ, Serrels B, Metcalf CA, 3rd, Sawyer TK, et al. Identification of Src-specific phosphorylation site on focal adhesion kinase: dissection of the role of Src SH2 and catalytic functions and their consequences for tumor cell behavior. Cancer Res. 2005;65:1335-42.

37. McLean GW, Carragher NO, Avizienyte E, Evans J, Brunton VG, Frame MC. The role of focal-adhesion kinase in cancer - a new therapeutic opportunity. Nat Rev Cancer. 2005;5:505-15.

38. Mitra SK, Hanson DA, Schlaepfer DD. Focal adhesion kinase: in command and control of cell motility. Nat Rev Mol Cell Biol. 2005;6:56-68.

39. Tai YL, Chen LC, Shen TL. Emerging roles of focal adhesion kinase in cancer. Biomed Res Int. 2015;2015:690690.

40. Joannes A, Grelet S, Duca L, Gilles C, Kileztky C, Dalstein V, et al. Fhit regulates EMT targets through an EGFR/Src/ERK/Slug signaling axis in human bronchial cells. Mol Cancer Res. 2014;12:775-83.

41. Di Florio A, Adesso L, Pedrotti S, Capurso G, Pilozzi E, Corbo V, et al. Src kinase activity coordinates cell adhesion and spreading with activation of mammalian target of rapamycin in pancreatic endocrine tumour cells. Endocr Relat Cancer. 2011;18:541-54.

42. Francois RA, Maeng K, Nawab A, Kaye FJ, Hochwald SN, Zajac-Kaye M. Targeting focal adhesion kinase and resistance to mTOR inhibition in pancreatic neuroendocrine tumors. J Natl Cancer Inst. 2015;107:div123.

7. FIGURE LEGENDS

Figure 1. Expression of DCLK1 in pancreatic neuroendocrine tumors (PNETs) and the human PNET cell line CM. Upper panels (A, B, and C) show HE and DCLK1 staining of a G2 grade PNET (case No. 4), and lower panels (D, E, and F) show HE and DCLK1 staining of a G2 grade PNET (case No.5), respectively. Strong and diffuse cytoplasmic expression of DCLK1 is observed in tumor cells. A, B, D, and E, magnification 100x; C and F, 400x. In western blot analysis, the DCLK1 expression is clearly found in CM cells (G), one of the three PNET cell lines available for experiments to date.

Figure 2. Overexpression of DCLK1 in QGP1 cells (QGP1-DCLK1 cells) shown by western blotting. EV, empty vector-transfected QGP1 cells (A). An increase of polygonal and spindle-shape cells is observed in the QGP1-DCLK1 cells (B). In a wound-healing assay, significantly greater migration ability is observed in the QGP1-DCLK1 cells compared to that of the control cells (C and D). Confirmation of siRNA-mediated knockdown of *DCLK1* expression in CM cells by western blotting. siNT, non-targeted (NT) siRNA-treated CM cells (E). Wound healing is retarded in *DCLK1*-silenced CM cells (CM-siDCLK1; F and G). Comprehensive gene expression analysis by cDNA microarray shows upregulated expression of the EMT-associated transcription factor *SLUG* in QGP1-DCLK1 cells compared the expression in EV cells (H). All data are expressed as mean ± SD. ※, $p < 0.01$, Mann-Whitney U test.

Figure 3. Validation of gene expression by qPCR. *SLUG* upregulation is observed as well as the upregulated expression of the mesenchymal markers *VIMENTIN* and *N-CADHERIN*. However, the expression of *E-CADHERIN* is not always significantly downregulated in this experiment (A). All data are expressed as mean ± SD. ※, $p < 0.01$, Mann-Whitney U test. In western blotting, corresponding changes in protein expression levels are confirmed in not only QGP1-DCLK1 cells but also BON1-DCLK1 cells (B). N-CAD, N-CADHERIN; VIM, VIMENTIN; and E-CAD, E-CADHERIN.

Figure 4. Xenograft PNET tumors in nude mice. Mice were sacrificed at day 42. QGP1-DCLK1 cells formed significantly larger xenograft tumors than QGP1-EV cells (A, B, and C). Tumor weight (g) is shown as mean ± SD. ※, $p < 0.01$, Mann-Whitney U test. Consistently, a significantly higher frequency of mitosis (arrows in D) is observed in the QGP1-DCLK1 tumor tissues stained with hematoxylin and eosin. HPF, high-power field. Data obtained from 6 random HPFs are expressed as mean ± SD. ※, $p < 0.01$, Mann-Whitney U test (E). A representative western blotting demonstrates that FAK and its downstream molecules, PAXILLIN, ERK1/2, AKT, and CYCLIN D1 are involved. Notably, Tyr^{925}-p-FAK, but not Tyr^{397}-p-FAK, was robustly

expressed in the QGP1-DCLK1 tumor tissues, accompanied by increased expression of PAXILLIN, p-ERK1/2, p-AKT, and CYCLIN D1 (F). Immunohistochemistry shows that the expression of the EMT regulator SLUG is increased in a representative QGP1-DCLK1 tumor tissue (G). All tumors examined (n=5) demonstrate that upregulation of both SLUG and Tyr^{925}-p-FAK is statistically significant in our scoring system. ※, $p < 0.01$, Mann-Whitney U test (G).

Figure 5. *DCLK1* knockdown downregulates Tyr^{925}-p-FAK and SLUG. Western blotting analysis showing that Tyr^{925}-p-FAK and SLUG protein expression is restored by 50 nM *DCLK1*-specific siRNA (siDCLK1; panel A). In DCLK1-positive CM cells, *DCLK1* silencing results in downregulation of SLUG and Tyr^{925}-p-FAK, and Tyr^{925}-p-FAK downregulation occurs earlier and is stronger (B).

Figure 6. FAK activation is upstream of SLUG. Silencing of *FAK* by siRNA in QGP1-DCLK1 cells leads to a clear downregulation of SLUG (A), and this effect is mimicked by treatment with 1 μM of LRRK2-IN-1 (LRRK2), a DCLK1 inhibitor (B), where loss of SLUG is through loss of Tyr^{925}-p-FAK in QGP1-DCLK1 cells. Note, total FAK expression is unaltered (B). Treatment with another small molecule XMD 8-92 results in decreased expressions of both Tyr^{925}-p-FAK and SLUG in a dosage-dependent manner, in not only QGP1-DCLK1 cells but also CM cells (C).

Figure 7. Cartoon for the proposed role of DCLK1 overexpression in human PNET. The findings obtained from this study suggest that DCLK1 and Tyr^{925}-p-FAK-mediated EMT involving p-ERK1/2 and SLUG upregulation plays a critical role in determining tumor cell behavior in PNETs. Such activation of FAK in the tumor may contribute to the increase in tumor size and cellular proliferation through upregulating the cell cycle driver CYCLIN D1.

Figure 1

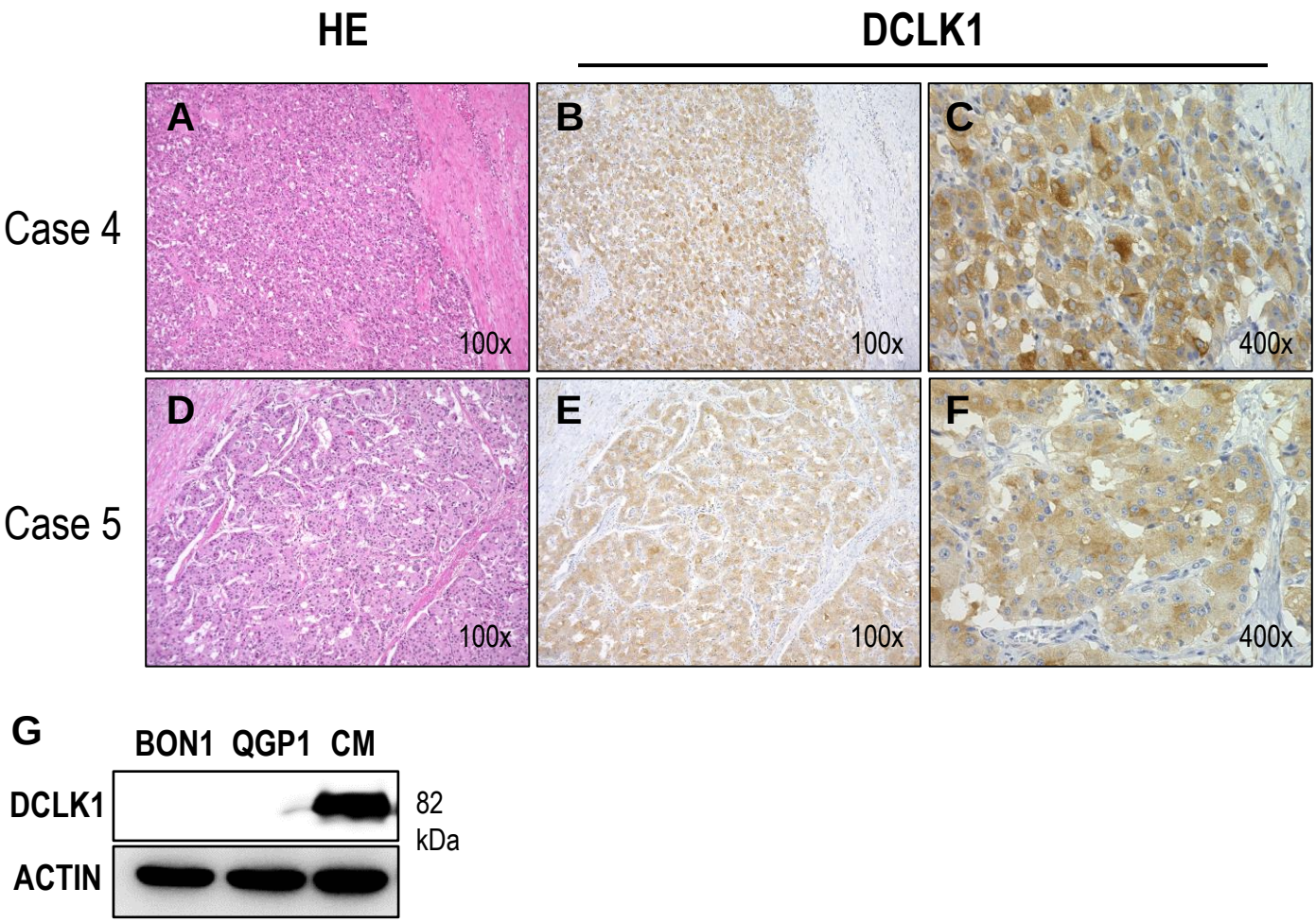
HE
DCLK1
Case 4
Case 5
A
B
C
D
E
F
100x
100x
400x
100x
100x
400x

G
BON1 QGP1 CM
DCLK1
ACTIN
82
kDa

Figure 2

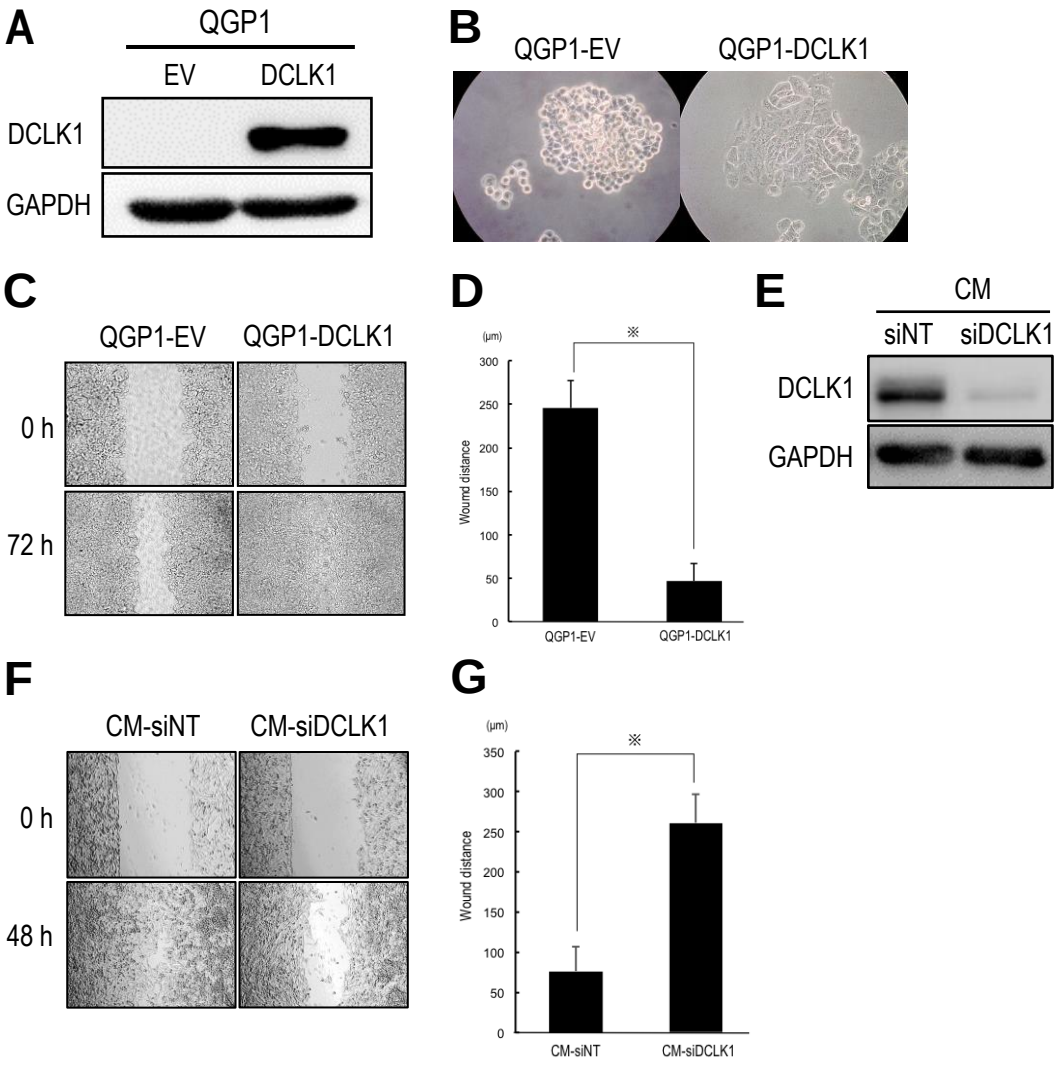
A
QGP1
EV
DCLK1
DCLK1
GAPDH
B
QGP1-EV
QGP1-DCLK1
C
QGP1-EV
QGP1-DCLK1
0 h
72 h
D
(μm)
※
Wound distance
300
250
200
150
100
50
0
QGP1-EV
QGP1-DCLK1
E
CM
siNT
siDCLK1
DCLK1
GAPDH
F
CM-siNT
CM-siDCLK1
0 h
48 h
G
(μm)
※
Wound distance
350
300
250
200
150
100
50
0
CM-siNT
CM-siDCLK1

Figure 3

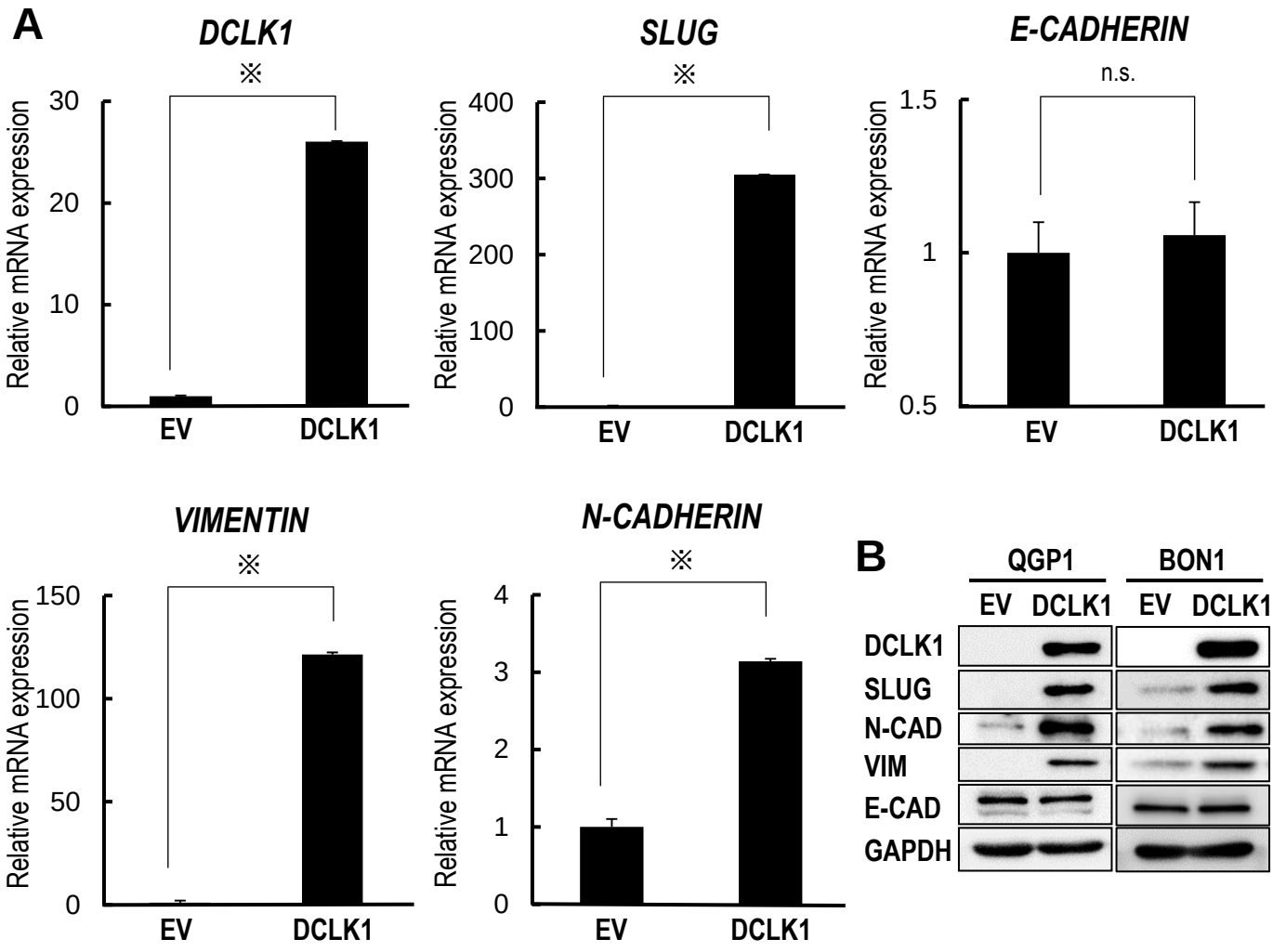
A
DCLK1
※
Relative mRNA expression
30
20
10
0
EV
DCLK1
SLUG
※
400
300
200
100
0
E-CADHERIN
n.s.
1.5
1
0.5
VIMENTIN
150
100
50
N-CADHERIN
4
3
2
1
B
QGP1
BON1
EV
DCLK1
DCLK1
SLUG
N-CAD
VIM
E-CAD
GAPDH

Figure 4

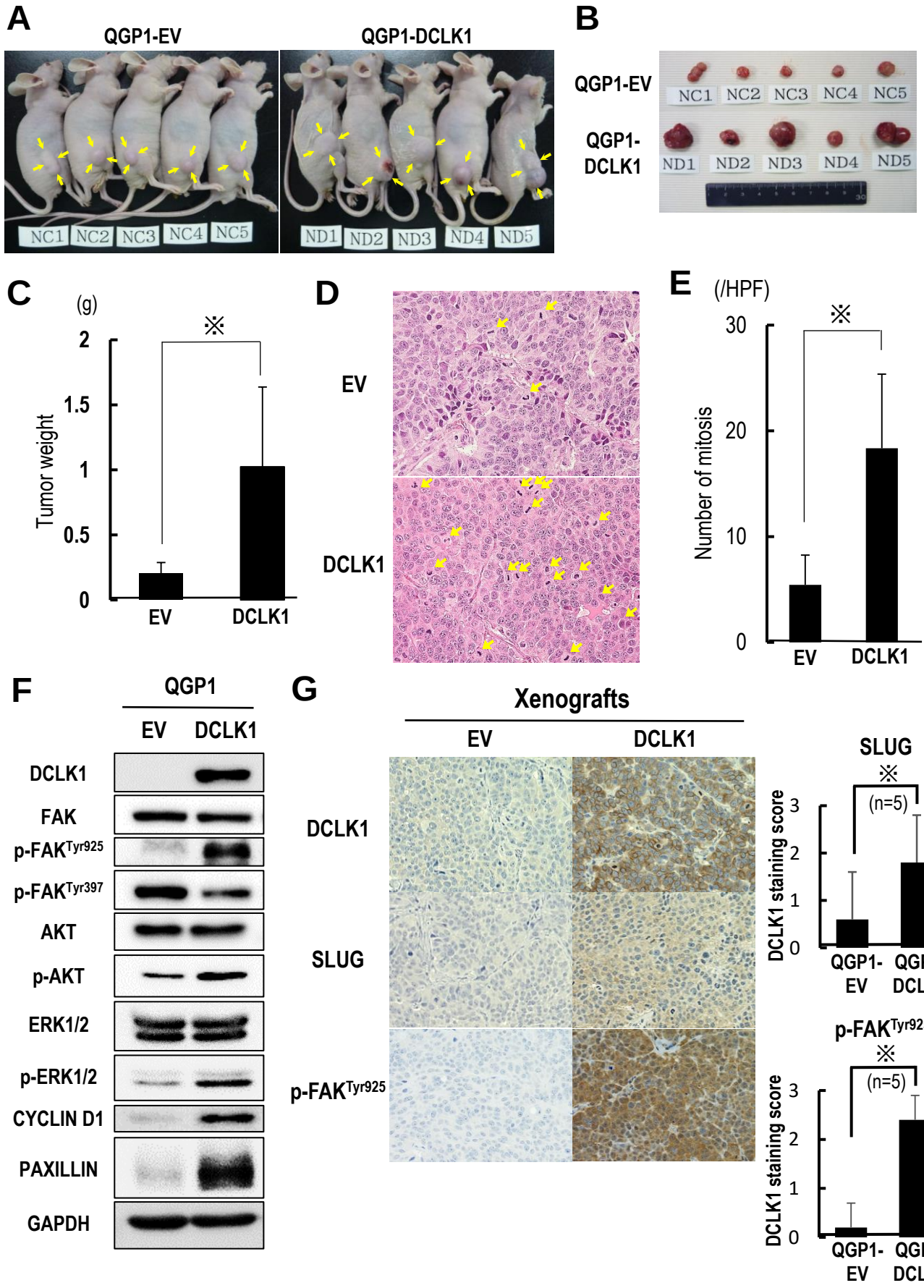
A
QGP1-EV
QGP1-DCLK1
NC1 NC2 NC3 NC4 NC5
ND1 ND2 ND3 ND4 ND5
B
QGP1-EV
QGP1-DCLK1
NC1 NC2 NC3 NC4 NC5
ND1 ND2 ND3 ND4 ND5
C
(g)
※
Tumor weight
2
1.5
1
0.5
0
EV
DCLK1
D
EV
DCLK1
E
(/HPF)
※
Number of mitosis
30
20
10
0
EV
DCLK1
F
QGP1
EV DCLK1
DCLK1
FAK
p-FAKTyr925
p-FAKTyr397
AKT
p-AKT
ERK1/2
p-ERK1/2
CYCLIN D1
PAXILLIN
GAPDH
G
Xenografts
EV
DCLK1
DCLK1
SLUG
p-FAKTyr925
SLUG
※
(n=5)
DCLK1 staining score
3
2
1
0
QGP1-EV
QGP1-DCLK1
p-FAKTyr925
※
(n=5)
DCLK1 staining score
3
2
1
0
QGP1-EV
QGP1-DCLK1

Figure 5

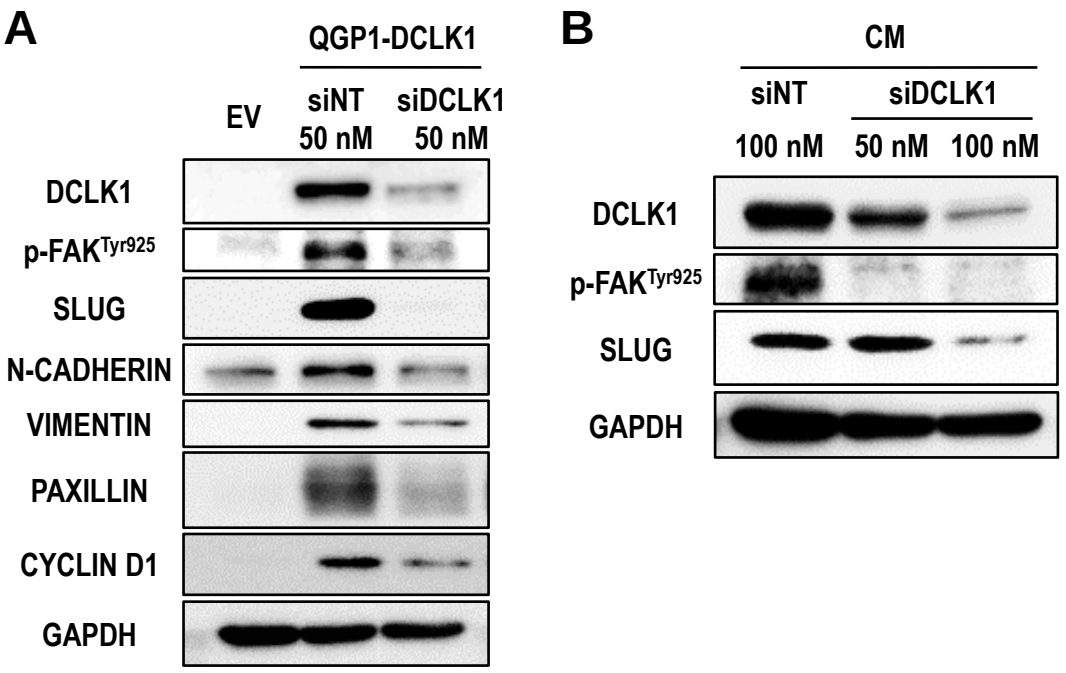
A
QGP1-DCLK1
EV
siNT
50 nM
siDCLK1
50 nM
DCLK1
p-FAK Tyr925
SLUG
N-CADHERIN
VIMENTIN
PAXILLIN
CYCLIN D1
GAPDH
B
CM
siNT
siDCLK1
100 nM
50 nM
100 nM
DCLK1
p-FAK Tyr925
SLUG
GAPDH

Figure 6

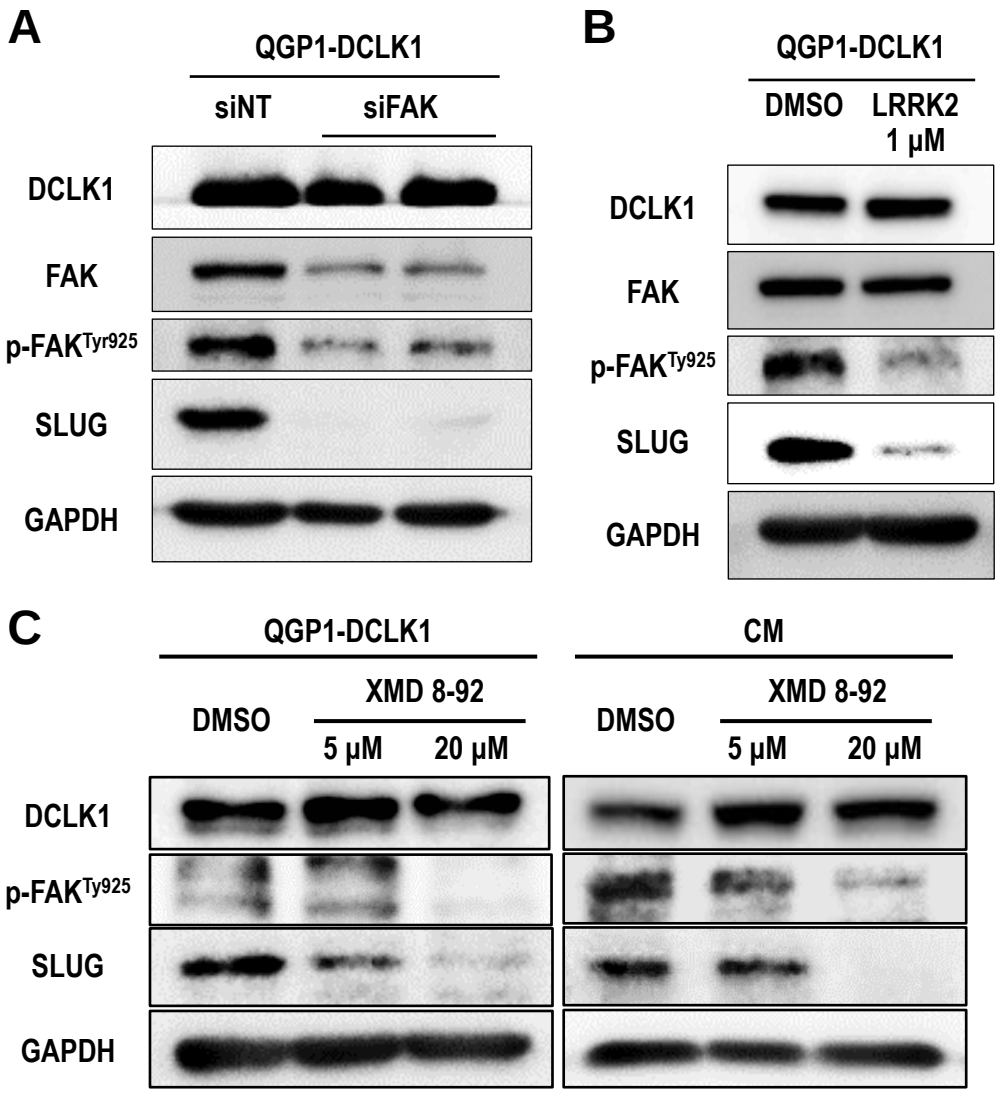
A
QGP1-DCLK1
siNT
siFAK
DCLK1
FAK
p-FAK Tyr925
SLUG
GAPDH
B
QGP1-DCLK1
DMSO
LRRK2 1 μM
DCLK1
FAK
p-FAK Ty925
SLUG
GAPDH
C
QGP1-DCLK1
CM
DMSO
XMD 8-92
5 μM
20 μM
DMSO
XMD 8-92
5 μM
20 μM
DCLK1
p-FAK Ty925
SLUG
GAPDH

Figure 7

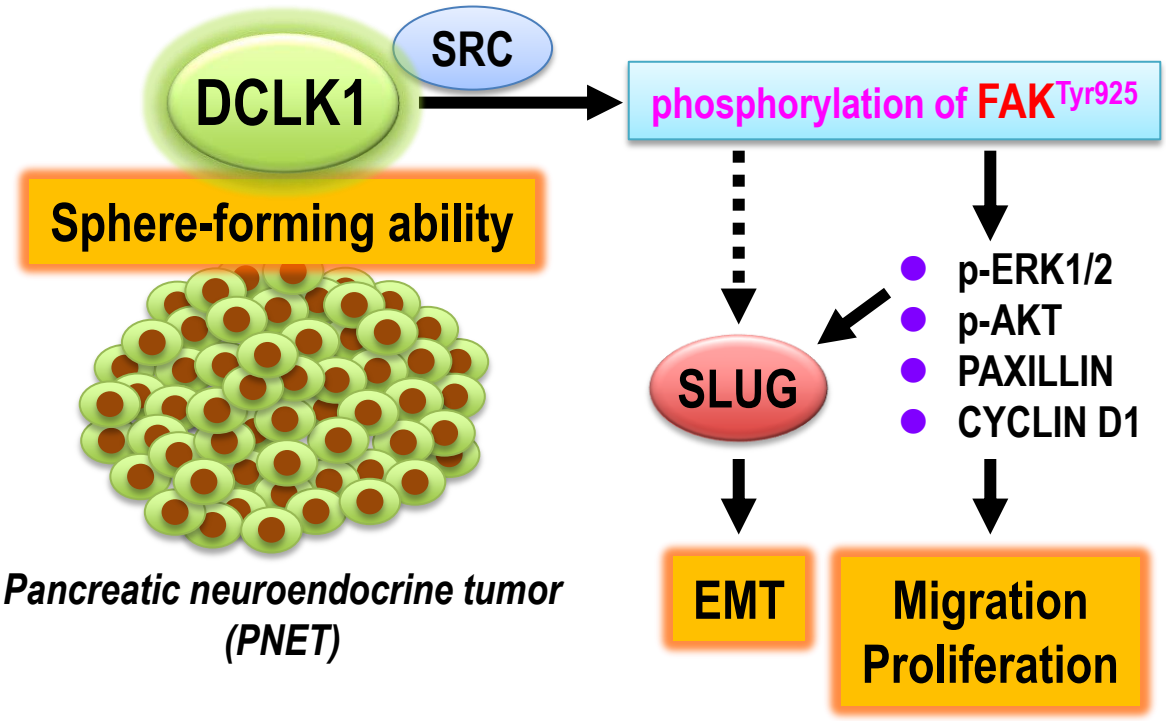
SRC
DCLK1
phosphorylation of FAK Tyr925
Sphere-forming ability
p-ERK1/2
p-AKT
PAXILLIN
CYCLIN D1
SLUG
EMT
Migration
Proliferation
Pancreatic neuroendocrine tumor
(PNET)

Table 1. Characteristics of patients and tumors

Sex	Male	8
	Female	7
Age (range) (years)		56 (17-80)
Tumor grade (G1/G2)		9/6
Long diameter of tumors (range) (mm)		30.2 (12-93)
Functional/Non-functional		3/12
Metastasis positive/negative		8/7

Table 2. Evaluation criteria for immunostaining

Score	0	1	2	3
Signal intensity	negative	mild	moderate	strong
Positive area (%)	0-10	11-60	61-100	

Table 3. List of antibodies used in this study

Antigen	Clone/type	Dilution	Antigen retrieval	Source
DCLK1	EPR6085	1:700	H	Abcam, Cambridge, UK
SYNAPTOPHYSIN	Z66	1:1	H	Invitrogen, Frederick, MD
CHROMOGRANIN A	DAK-A3	1:400	H	DakoCytomation, Glostrup, Denmark
CD56	1B6	1:200	H	Leica Microsystems, Newcastle, UK
SLUG	(Polyclonal)	1:700	H	Abcam, Cambridge, UK
Ki-67	MIB-1	1:200	H	DakoCytomation, Glostrup, Denmark

H, heat-activated

Table 4. Immunoreactivity scores for DCLK1 and positivity for known neuroendocrine markers

No.	Age	Sex	Location	Grade	Size (mm)	Function	DCLK1	Cg A	CD56	SYP	MIB1
1	53	F	BT	G1	70×36	-	3	+	-	+	<2%
2	70	M	BT	G2	28×20	-	5	+	+	+	<2%
3	77	F	H	G1	14×12	-	3	+	+	+	<2%
4	51	F	T	G2	93×70	-	5	+	+	+	5%
5	21	M	T	G2	32×22	-	5	+	+	+	3-5%
6	64	F	T	G2	20×15	+	4	+	+	+	10%
7	80	M	BT	G1	12×10	-	3	-	+	+	<2%
8	59	F	H	G1	18×17	-	5	+	+	+	<2%
9	48	M	BT	G2	32×22	-	5	+	-	+	8-10%
10	65	M	H	G1	25×25	-	5	+	-	+	2%
11	52	F	B	G2	25×35	-	5	+	-	+	3-5%
12	17	M	B	G1	20×18	+	5	+	-	-	<2%
13	56	M	B	G1	32×38	-	3	+	+	+	<2%
14	57	M	T	G1	14×12	+	5	+	+	+	<2%
15	71	F	B	G1	29×24	-	5	-	-	+	<2%

H, B, and T in Location indicate head, body, and tail of the pancreas, respectively.

LEGENDS FOR SUPPLEMENTARY FIGURES

Supplementary Figure 1S. Negative control for immunohistochemistry. Rabbit IgG (Santa Cruz Biotechnology, CA; Cat. #sc-2027) was used in place of the primary antibody for DCLK1.

Supplementary Figure 2S. Comparison of DCLK1 immunostaining scores between primary PNETs and metastatic sites (lymph nodes) in four cases. n.s., not significant.

Supplementary Figure 3S. Expression of DCLK1 in primary liver NET (LNET) tissues. DCLK1 is expressed as a full-length isoform (82 kDa) in LNET tissues (A). NT indicates non-tumorous liver tissue surrounding the tumor (T). The used antibody reacts with DCLK1 in LNET tissues obtained from four patients (Case 1-4) (B). Strong and diffuse expression of DCLK1 is observed in LNET tissues. Surrounding hepatocytes (arrow in Case 1) are negative for the expression.

Supplementary Figure 4S. cDNA microarray analysis to compare DCLK1-overexpressing QGP1 cells (DCLK1) with empty vector-transfected control cells (EV).

Supplementary Figure 5S. Sphere formation assay. (A) The area of the cell spheres is measured using a microscope equipped with digital cell counting software (left panels, phase-contrast images; right, digital images). (B) Graph shows significantly larger area/well in QGP1-DCLK1 cells than control cells. ※, $p < 0.01$, Mann-Whitney U test.

Supplementary Figure 1S

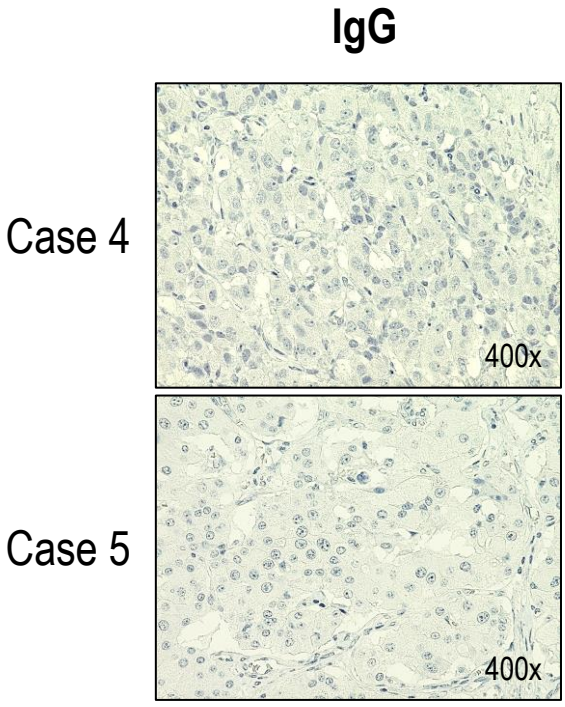

Supplementary Figure 2S

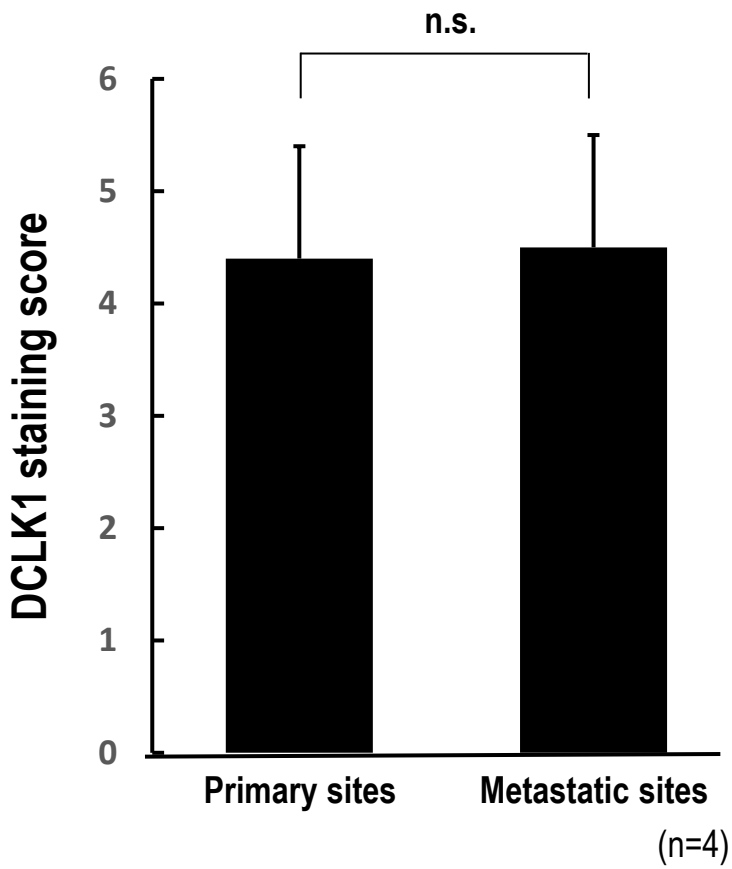

Supplementary Figure 3S

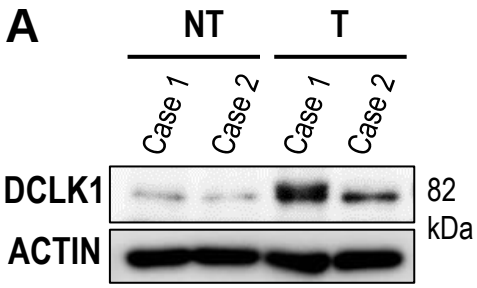

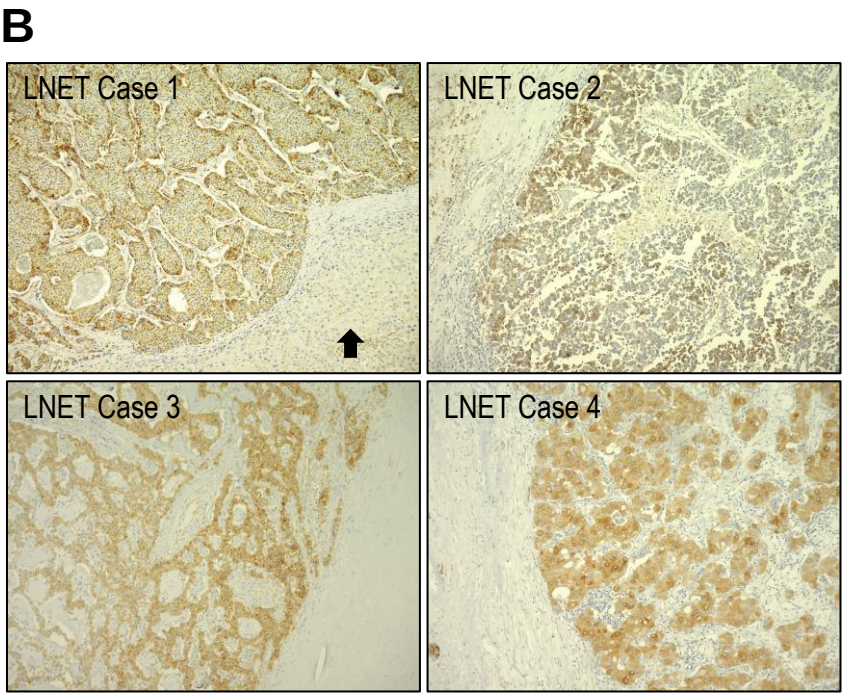

Supplementary Figure 4S

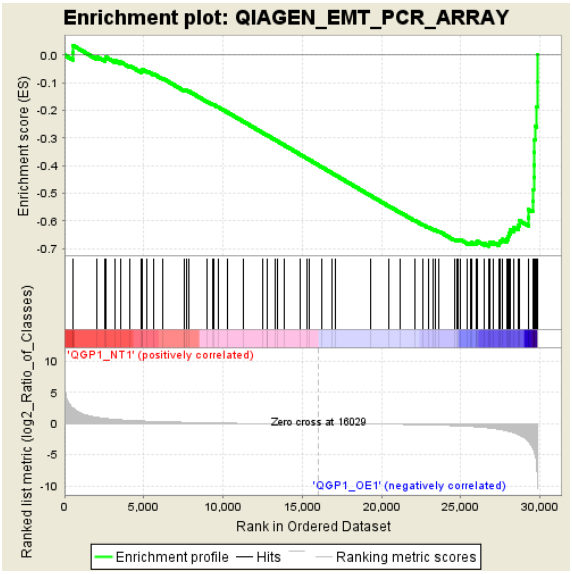

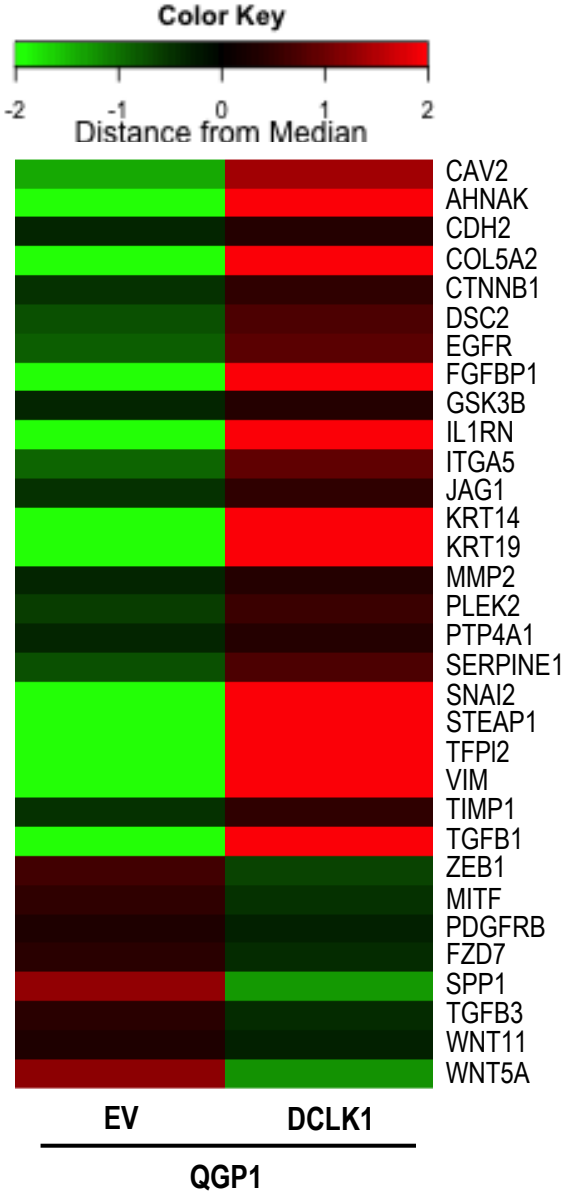

Supplementary Figure 5S